

# Hydrodynamical Adaptive Mesh Refinement Simulations of Disk Galaxies

Brad K. Gibson<sup>1†</sup>, Stéphanie Courty<sup>1</sup>, Patricia Sánchez-Blázquez<sup>1</sup>,  
 Romain Teyssier<sup>2</sup>, Elisa L. House<sup>1</sup>,  
 Chris B. Brook<sup>3</sup>, and Daisuke Kawata<sup>4</sup>

<sup>1</sup>Centre for Astrophysics, University of Central Lancashire, Preston, PR1 2HE, UK  
 email: [bkgibson@uclan.ac.uk](mailto:bkgibson@uclan.ac.uk)

<sup>2</sup>Service d'Astrophysique, CEA Saclay, Batiment 709, 91191 Gif sur Yvette, France

<sup>3</sup>Department of Astronomy, University of Washington, Seattle, WA, 98195, USA

<sup>4</sup>Carnegie Observatories, 813 Santa Barbara St., Pasadena, CA, 91101, USA

**Abstract.** To date, fully cosmological hydrodynamic disk simulations to redshift zero have only been undertaken with particle-based codes, such as **GADGET**, **Gasoline**, or **GCD+**. In light of the (supposed) limitations of traditional implementations of smoothed particle hydrodynamics (SPH), or at the very least, their respective idiosyncrasies, it is important to explore complementary approaches to the SPH paradigm to galaxy formation. We present the first high-resolution cosmological disk simulations to redshift zero using an adaptive mesh refinement (AMR)-based hydrodynamical code, in this case, **RAMSES**. We analyse the temporal and spatial evolution of the simulated stellar disks' vertical heating, velocity ellipsoids, stellar populations, vertical and radial abundance gradients (gas and stars), assembly/infall histories, warps/lopsideness, disk edges/truncations (gas and stars), ISM physics implementations, and compare and contrast these properties with our sample of cosmological SPH disks, generated with **GCD+**. These preliminary results are the first in our long-term Galactic Archaeology Simulation program.

**Keywords.** galaxies: formation, galaxies: evolution, methods: n-body simulations

## 1. Introduction

The ability to form and evolve (correctly!) a disk galaxy with the aid of massively parallel computers and optimised algorithms remains an elusive challenge for astrophysicists. Ameliorating the non-physical effects associated with overcooling, overmerging, angular momentum loss, and the capture of accurate phenomenological prescriptions for the sub-grid physics governing galaxy evolution (star formation, feedback, etc.) has been achieved through rapid advancements in both hardware and software algorithms, but their complete elimination has yet to be realised.

Fully self-consistent cosmological hydrodynamic simulations of Milky Way-like disk galaxies, with sufficient resolution ( $\lesssim 500$  pc) to decompose and analyse various galactic sub-components (eg. halo, bulge, and thin + thick disks) have only really appeared over the past  $\sim 5$  years (Sommer-Larsen et al. 2003; Abadi et al. 2003; Governato et al. 2004, 2007; Robertson et al. 2004; Bailin et al. 2005; Okamoto et al. 2005).

A common thread linking these studies is the use of a particle-based approach to representing and solving the equations of hydrodynamics - usually through the use of a smoothed particle hydrodynamics (SPH) code, such as **GADGET**, **Gasoline**, or **GCD+**. Where there is no disputing the impact that SPH has had on the field, it is important to be aware of both the strengths *and* weaknesses of any specific approach - as O'Shea et al.

† <http://www.uclan.ac.uk/~bkg/>

(2005) and Agertz et al. (2007) have shown, both subtle *and* overt differences can be introduced when employing a particle-based, as opposed to a mesh-based (or grid-based) approach (and *vice versa*), when simulating galaxy formation and evolution.

To address these concerns, we have initiated a long-term Galactic Archaeology Simulation programme aimed at complementing the aforementioned particle-based studies (including our own) with a comprehensive suite of simulations generated with a grid-based N-body + hydrodynamical code employing adaptive mesh refinement (AMR) - our software tool of choice has been **RAMSES** (Teyssier 2002). *These simulations represent (to our knowledge) the first to be generated through to redshift zero, with a grid code, within a fully cosmological and hydrodynamic framework.*†

In this contribution, we provide a brief summary of the methodology adopted, and highlight several *preliminary* results associated with our analyses of the simulations' disk kinematics, chemistry, disk edges / truncations, and assembly / infall histories.

## 2. Methodology

From a parent  $20 h^{-1}$  Mpc  $\Lambda$ CDM collisionless particle simulation, several representative  $\sim 5-8 \times 10^{11} M_\odot$  halos were identified for higher-resolution re-simulation with the full baryonic physics capabilities of **RAMSES**. Unlike previous studies, we placed essentially no *a priori* restrictions during the halo selection process - ie, we did *not* purposefully select isolated, median-spin halos, with particularly quiescent assembly histories, in an attempt to bias the selection towards a "Milky Way-like" halo.

The parent dark matter simulation was re-centred on the halo of interest with now three nested areas of different mass resolution. Only the central  $512^3$  coarse grid was then refined, up to 7 additional levels, with the full suite of baryonic physics included (eg. star formation, blast-wave supernovae feedback parametrisation, chemical enrichment, UV background, metal-dependent cooling, etc.), resulting in a formal spatial (baryonic mass) resolution of 435 pc ( $10^6 M_\odot$ ) at  $z=0$ .‡ The resolution is roughly a factor of two better than that employed in our earlier SPH work (Brook et al. 2004; Bailin et al. 2005).

## 3. Basic Characteristics

Our first two  $\sim L^*$  disks (Ramses1 and Ramses2, respectively) both ended as fast-rotating massive ( $7.6 \times 10^{11} M_\odot$  and  $5.5 \times 10^{11} M_\odot$ , respectively) galaxies in low-spin ( $\lambda=0.02$ ) halos. Bandpass-dependent bulge-to-disk (B/D) decompositions show, not surprisingly, B/D ratios in the range of  $\sim 0.4-0.8$ , signatures of the same overcooling / overcentralisation "problems" which plague traditional SPH disk simulations. The stellar bulge has a  $V/\sigma \sim 0.5$ , reflecting its  $\sim 70$  km/s rotation.¶ That said, the simulated I-band images (edge-on and face-on) for Ramses1 (middle and right panels of Fig 1) are more than encouraging. The left-most panel of Fig 1 shows the gas density distribution (different projection); the tell-tale warp can be traced to a neighbouring satellite.

The overall star formation histories for the two **RAMSES** disks are not dissimilar to those associated with our two **GCD+** SPH disks - GCD1 (Bailin et al. 2005: fully-cosmological, using the Abadi et al. (2003) initial conditions; GCD2 (Brook et al. 2004) semi-cosmological (Fig 2). Each shows the tell-tale peak in star formation between  $z \approx 2-4$ , with an associated exponential decline over the past  $\sim 10$  Gyrs to a present-day rate of  $\sim 1-2 M_\odot/\text{yr}$ .

† The beautiful simulations of Ceverino & Klypin (2008), generated with the **ART** grid code were not (again, to our knowledge) run to redshift zero.

‡ At the time of writing, an additional level of refinement has been completed, taking the resolution to  $\sim 200$  pc.

¶ Similar to that of the Milky Way, although we should emphasise again that Ramses1 is not supposed to be a one-to-one "clone" of the Milky Way.

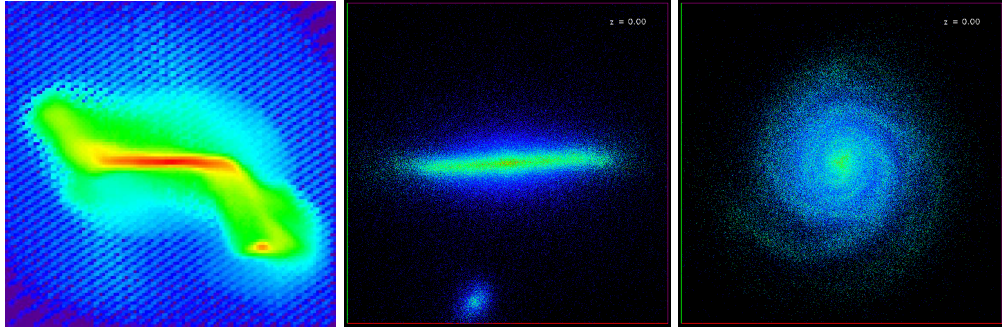


**Figure 1.** Gas (left) and stellar light (I-band: middle and right) distributions ( $60 \times 60$  kpc) for the Ramses1 disk galaxy.

In detail, the star formation histories of both **RAMSES** disks compare very favourably to that inferred from semi-numerical Galactic Chemical Evolution models, for the Milky Way as a whole; indeed, Ramses2 and the Milky Way model of Fenner *et al.* (2005), are extremely similar in their global star formation histories.

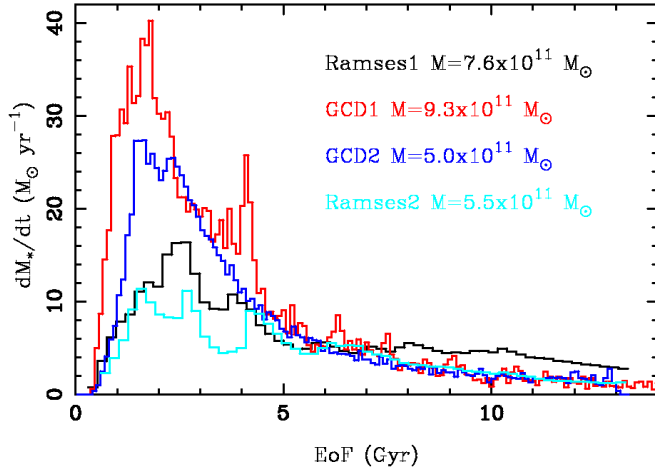


**Figure 2.** Time evolution of the star formation rate (within 30 kpc) for the two **RAMSES** disks described here, alongside those for our two earlier **GCD+** SPH disk galaxies.

#### 4. Chemistry

Our current implementation of chemistry within **RAMSES** is restricted to the global metal content ( $Z$ ), under the assumption of the instantaneous recycling approximation. We are in the midst of porting to **RAMSES** the more sophisticated chemical evolution modules from our **GEtool** (95 isotopes; 34 elements: Fenner *et al.* 2005) and **GCD+** (9 isotopes; 9 elements: Kawata & Gibson 2003) codes. Having said that, there are useful and important chemical characteristics which can be extracted and examined, including the degree of azimuthal variation in the global metallicity (both stellar and gas-phase) and the overall metallicity gradients in the thin and thick stellar disk components.

For example, within the Milky Way, the local peak-to-peak scatter in the gas-phase abundances is  $\sim 0.4$  dex (Cescutti *et al.* 2007; Fig 3). Examining the Ramses1 simulation, we find a comparable azimuthal variation in the gas metallicities ( $\sim 0.2 \rightarrow -0.5 Z_{\odot}$ ) at radii of 8–10 kpc. We find a mid-plane (thin disk) abundance gradient of  $dZ/dR \sim -0.03$  dex/kpc,

comparable to that observed locally (Cescutti et al.; Tbl 5) and consistent with an “inside-out” disk growth scenario (Fenner et al. 2005); the gradient in the thick disk is a factor of two shallower over the same galactocentric distance.

## 5. Kinematics

One of the pillars of Galactic Archaeology has been the suggestion that within the Milky Way, vertical disk heating saturates at  $\sigma_z \sim 20$  km/s for stars of ages  $\sim 2-10$  Gyrs (Quillen & Garnett 2001); for older stars, a discrete jump to  $\sigma_z \sim 45$  km/s is apparent which could be a signature of the thick disk. These conclusions have been questioned by Holmberg et al. (2007), who claim that the evidence instead supports a picture in which the disk has undergone continual heating throughout this period. These opposing scenarios are represented in schematic form by the yellow lines in Fig 3.

Our semi-cosmological models (Brook et al. 2004) appear to be more consistent with the “disk saturation” scenario (see the blue GCD2 curve of Fig 3), with the older, hotter, stars being associated with the *in situ* formation of the thick disk during the intense gas-rich merger phase at high-redshift. The cosmological disks (both the new **RAMSES** pair, and our Bailin et al. 2005 SPH galaxy) though appear to be more consistent (or at least not inconsistent) with the “continual heating” scenario (see the Ramses1, Ramses2, and GCD1 curves of Fig 3). There are a large number of caveats that need to be noted here, each of which will be explored in a future paper: (i) the cosmological models capture late-time infall more accurately than the semi-cosmological models; (ii) the Ramses2 model, while showing evidence for continual disk heating, also shows evidence of an “impulsive” step for stars older than  $\sim 10$  Gyrs, suggesting a hybrid picture might be more appropriate for this galaxy; (iii) again, the cosmological disks were not chosen to be Milky Way “clones”, so one must be careful not to overinterpret the simulations. Regardless, it is fascinating to see the four simulations filling the area between the two extrema; we are expanding our simulation suite, in order to explore the range of heating scenarios, and its association with assembly history, environment, and mass.

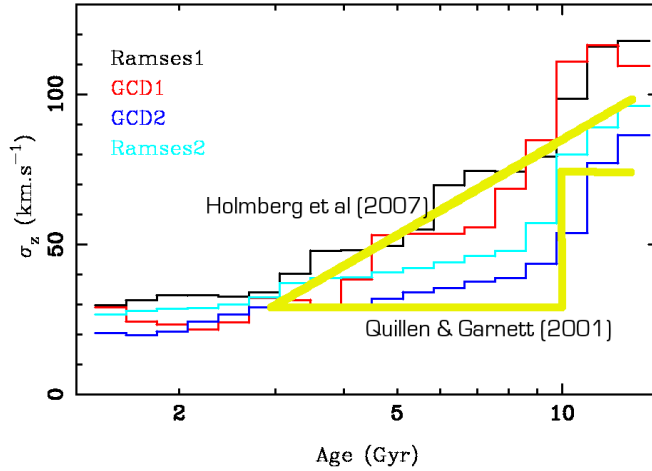


**Figure 3.** Age-velocity dispersion relation in the vertical direction for “local” disk stars in our suite of **RAMSES** and **GCD+** simulations. The suggested behaviour in the solar neighbourhood under the “disk saturation” (Quillen & Garnett 2001) and “continual heating” (Holmberg et al. 2007) scenarios are shown in schematic form.

We can go one step further and examine the spatial variation of  $\sigma_z$  (over  $\sim 1-4$  disk scale lengths) for intermediate-age stars (bottom right panel of Fig 5). The exponential

decline observed is consistent with that observed by Herrmann & Ciardullo (2008) in six nearby face-on galaxies. This is the expected behaviour for disks with constant M/L; the relatively high dispersions seen in the simulations (and in the observational data) beyond  $\sim 2-3$  scale lengths is likely due to the combination of disk heating and flaring.

Finally, we note in passing that the thick disks in our simulations lag those of their respective thin disks, much like the spirals in Yoachim & Dalcanton (2008) (by  $\sim 70-100$  km/s at galactocentric radii of 8–10 kpc and 3–6 kpc above the mid-plane) This is encouraging, but we next need to explore how this scales with mass (cf. the mass-dependent lag claimed by Yoachim & Dalcanton 2008), whether the thick disk scale lengths are consistently greater than those of the thin disk (Yoachim & Dalcanton 2006), and whether these are independent of environment, as claimed by Santiago & Vale (2008). Our full suite of simulations will be brought to bear on these problems.

## 6. Disk Edges / Truncation

### 6.1. Gas Disks

The Ramses1 disk has been simulated with a range of ISM physics treatments, represented by models with and without a polytropic equation of state. Taking our simulation without the polytrope, we examined the distribution of both the neutral and ionised gas of the disk (see also Fig 1). Ramses1 possesses a lopsided HI disk with a truncation/break near 19 kpc, where the HI column density is  $\sim 2 \times 10^{19}$  cm $^{-2}$  (red curve of Fig 4), consistent with that observed by the THINGS team (Portas *et al.* 2008). Admittedly, the break is not as clear as that observed empirically (Portas *et al.*; Fig 3), but that reflects the fact that we have azimuthally averaged over  $2\pi$  radians, as opposed to splitting into twelve  $\pi/6$  segments and aligning at the “break”; as such, the lopsidedness “smears” the break in Fig 4 from 19 kpc to a range of radii spanning 19–26 kpc. The ionised disk extends  $\sim 30-50\%$  beyond the neutral disk, before being “lost” in the background corona, similar to that observed (Bland-Hawthorn *et al.* 1997).

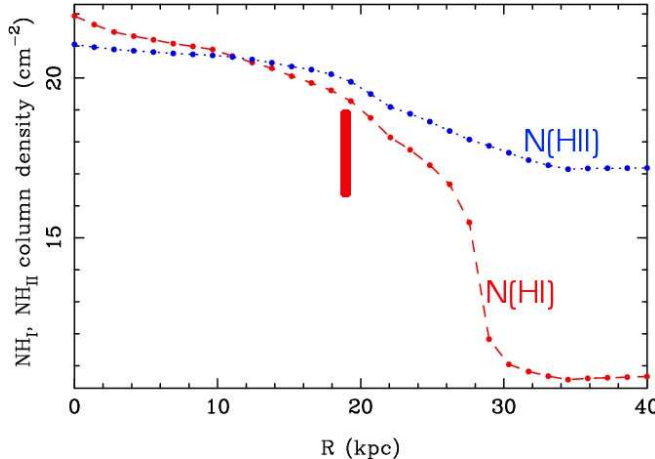


**Figure 4.** Neutral and ionised gas density distributions for the “no polytrope” simulation of Ramses1. The edge of the HI disk occurs near 19 kpc (vertical line), but is smeared out to  $\sim 26$  kpc by having averaged azimuthally over  $2\pi$  radians.

### 6.2. Stellar Disks

The origin of the apparent truncations to the exponential disks seen in the surface brightness distributions of spirals both locally and at high- $z$  is one of the most exciting areas of

disk galaxy “astrophysics” today (eg. Bakos et al. 2008 (B08); Roskar et al. 2008 (R08); and many references therein). The relative roles of star formation thresholds and radial migration / re-distribution of stars due to secular effects remains hotly debated.

In Fig 5 (ignoring the bottom right panel, which refers only to § 5), we show a series of panels, based on our analysis of the Ramses1 simulation, which should be examined beside the idealised simulation of R08 (Fig 1) and the observational data of B08 (Fig 1). There are a number of similarities, and tantalising differences, between the various datasets.

First, the two upper left panels show that while a break is seen at  $\sim 10$  kpc in both the B- and K-band, there is little (if any) evidence for a break in the stellar surface density. In addition, the bottom middle panel shows the disk colour becomes blue with increasing radius prior to the break, but becomes redder beyond it. Each of these are in agreement with the inferences derived empirically by B08; this is also more-or-less in agreement with the conclusions derived by R08 from a non-cosmological (but higher resolution) simulation, although R08 find a break in the stellar surface density that we (and B08) do not. Much like the colour becoming redder beyond the break, we find an associated increase in the stellar age of these stars (bottom left panel), in agreement with R08.

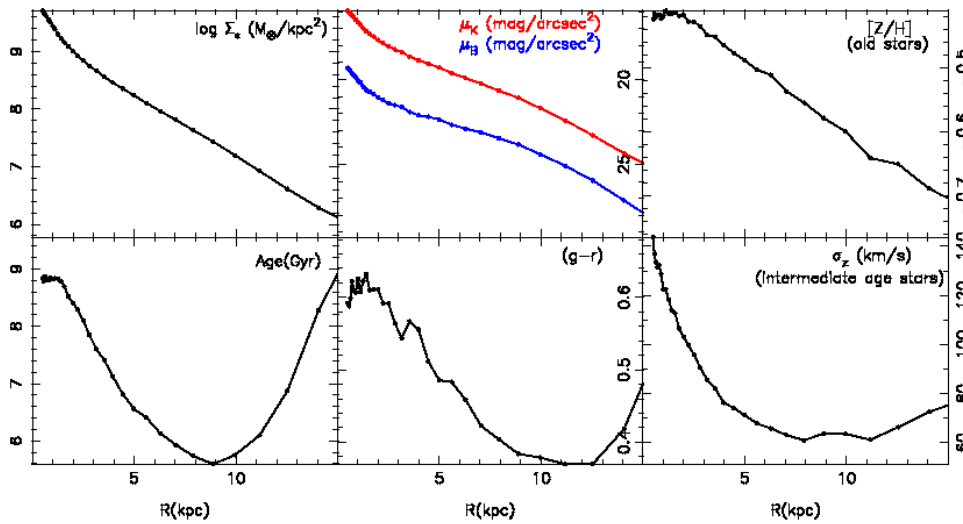


**Figure 5.** Radial stellar surface density (upper left), brightness (upper middle), mass-weighted metallicity for old stars (upper right), mass-weighted age (bottom left), colour (middle bottom), and vertical velocity dispersion (bottom right: § 5) for the Ramses1 stellar disk.

Within the picture proposed by R08, the stars beyond the break today are primarily old, born primarily in the inner disk (somewhat inside the break radius at the time of birth), and migrated to the outer disk due to various secular re-distribution effects. We are exploring the veracity of this elegant suggestion with our suite of cosmological simulations; there is migration within the cosmological simulation, but the relative contribution of secular re-distribution, *in situ* formation,† and satellite debris,‡ beyond the break, needs careful examination.

† Which does occur, as there is a not insignificant number of gas cells in the disk with densities in excess of the  $0.1 \text{ cm}^{-3}$  star formation threshold.

‡  $\sim 50\%$  of stars beyond the break formed since  $z=2.3$ , the highest redshift for which we could accurately identify and align the disk; of this fraction,  $\sim 30\%$  formed at galactocentric radii in excess of the present-day break; indeed, much of this disk “debris” formed in satellites distributed fairly uniformly in radius within the virial radius of the host halo.

One issue which needs to be addressed, which has perhaps not been appreciated previously, is that shown in the upper right panel to Fig 5. Here, we show the metallicity gradient of the old ( $>7$  Gyrs) stars in our Ramses1 simulation. From the bottom left panel, we see that the outer disk stars are old; from the upper right panel, we see that they are also relatively metal-poor; in and of itself, this seems consistent with R08. The potential problem which arises is that from the upper right panel, we also see that stars of the same age in the inner disk are a factor of two more metal-rich. *One must ask why it is that old metal-poor stars from the inner disk get re-distributed to the outer disk, but old metal-rich stars of the same age from the inner disk do not get re-distributed.* We need to examine the metallicity distribution functions as a function of space and time within the simulations (both our's and those of R08) to better understand the situation.

## 7. Gas Accretion / Infall

We defer a detailed discussion of the gas accretion history to the future, but felt it worth noting here that we have measured the spatial and temporal infall of cold, warm, and hot gas both into the halo as a whole and onto the disk itself. For Ramses1, the flux of gas across a sphere of radius 30 kpc since redshift  $z \sim 2$  is  $\sim 1.5 - 0.5 M_{\odot}/\text{yr}$ ; this can be contrasted with the inferred infall within semi-numerical Galactic Chemical Evolution models: for example, for our Milky Way model described in Fenner *et al.* (2005), averaging over the entire disk, for the same redshift range, results in a predicted infall rate of  $\sim 5 - 1 M_{\odot}/\text{yr}$ . We can also determine the metallicity distribution of this infalling gas; for this particular 30 kpc surface at  $z=0$ ,  $\langle Z_g \rangle \sim 0.02 Z_{\odot}$ , with essentially no component in excess of  $\sim 0.05 Z_{\odot}$ , again consistent with the Fenner *et al.* semi-numerical models (which assume the infalling gas is  $\lesssim 0.1 Z_{\odot}$ ). We have also laid virtual slabs  $\pm 6$  kpc above and below the mid-plane of the simulated disk and measured the vertical gas flux through these surfaces, finding a rate of  $\sim 1 M_{\odot}/\text{yr}$ . We have conducted the same experiment with virtual slabs at  $\pm 1$  kpc above/below the plane, and found fluxes  $\sim 10 - 50 \times$  greater, reflecting the much greater “ISM circulation flux” near the plane dominating over the flux from cosmological infall, consistent with observations.

## 8. Summary and Future Directions

We have realised (to the best of our knowledge) the first fully self-consistent cosmological hydrodynamic disk simulations to  $z=0$  with a mesh code; the resolution attained is 435 pc. Several preliminary results include:

- the saturated vertical disk heating seen in semi-cosmological SPH simulations has not yet been clearly replicated in our cosmological simulations;
- the neutral gas disks show “edges” at comparable column densities to those observed; ionised gas disks extend beyond the neutral gas, again in agreement with those observed;
- the stellar surface brightness profiles show “breaks” in the exponential profiles, with associated increases (reddening) in the age (colour) of the stellar populations beyond the break, in agreement with observation; little evidence is seen for an associated break in the stellar surface density profile, also as inferred from observations; stars of the same age beyond and interior to the break do not appear to have the same metallicity, which may prove problematic for radial migration scenarios;
- gas accretion is not smooth, but does appear to be more-or-less “inside-out”;
- the disk-halo “circulation flux” is  $\sim 10-50 \times$  that of the “infalling flux” (again, consistent with the broad numbers associated with the Milky Way).

Beyond the analysis of the extant simulations, we have a number of planned enhancements, including full chemical evolution / tagging, a ten-fold increase in the number of

simulations (to examine scaling relations, environmental dependencies, and assembly history variations), a range of ISM physics implementations (various polytropic equations of state, blast wave parametrisations), quantifying warp and lopsidedness statistics (Mapelli et al. 2008), 2d IFU Lick index-style maps, dusty radiative transfer, high-velocity clouds, radial gas flows, and detailed SPH vs AMR comparisons with identical initial conditions.

## Acknowledgements

The support of the UK's Science & Technology Facilities Council (ST/F002432/1) and the Commonwealth Cosmology Initiative are gratefully acknowledged. We also wish to thank Ignacio Trujillo and Judit Bakos for their guidance. Simulations and analyses were carried out on COSMOS (the UK's National Cosmology Supercomputer) and the University of Central Lancashire's High Performance Computing Facility. The parent N-body simulation was performed within the framework of the Horizon collaboration (<http://www.projet-horizon.fr>).

## References

Abadi, M.G., Navarro, J.F., Steinmetz, M. & Eke, V.R. 2003, *ApJ*, 591, 499  
 Agertz, O., Moore, B., Stadel, J., et al. 2007, *MNRAS*, 380, 963  
 Bailin, J., Kawata, D., Gibson, B.K., et al. 2005, *ApJ*, 627, L17  
 Bakos, J., Trujillo, I. & Pohlen, M. 2008, *ApJ*, 683, L103  
 Bland-Hawthorn, J., Freeman, K.C. & Quinn, P.J. 1997, *ApJ*, 490, 143  
 Brook, C.B., Kawata, D., Gibson, B.K. & Freeman, K.C. 2004, *ApJ*, 612, 894  
 Cescutti, G., Matteucci, F., Francois, P. & Chiappini, C. 2007, *A&A*, 462, 943  
 Ceverino, D. & Klypin, A. 2008, *ApJ*, submitted  
 Fenner, Y., Murphy, M.T. & Gibson, B.K. 2005, *MNRAS*, 358, 468  
 Governato, F., Mayer, L., Wadsley, J. et al. 2004, *ApJ*, 607, 688  
 Governato, F., Willman, B., Mayer, L., et al. 2007, *MNRAS*, 374, 1479  
 Herrmann, K.A. & Ciardullo, R. 2008, in: J.G. Funes & E.M. Corsini (eds.), *Formation and Evolution of Galaxy Disks* (ASP Conf Ser), in press  
 Holmberg, J., Nordström, B. & Anderson, J. 2007, *A&A*, 475, 519  
 Kawata, D. & Gibson, B.K. 2003, *MNRAS*, 346, 135  
 Mapelli, M., Moore, B. & Bland-Hawthorn, J. 2008, in: J. Anderson, J. Bland-Hawthorn & B. Nordström (eds.), *The Galaxy Disk in Cosmological Context* (CUP), in press  
 Okamoto, T., Eke, V.R., Frenk, C.S. & Jenkins, A. 2005, *MNRAS*, 363, 1299  
 O'Shea, B.W., Nagamine, K., Springel, V., Hernquist, L. & Norman, M.L. 2005, *ApJS*, 160, 1  
 Portas, A., Brinks, E., Usero, A., et al. 2008, in: J. Anderson, J. Bland-Hawthorn & B. Nordström (eds.), *The Galaxy Disk in Cosmological Context* (Cambridge University Press), in press  
 Quillen, A.C. & Garnett, D.R. 2001, in: J.G. Funes & E.M. Corsini (eds.), *Galaxy Diks and Disk Galaxies* (ASP Conf Ser), p. 87  
 Robertson, B., Yoshida, N., Springel, V. & Hernquist, L. 2004, *ApJ*, 606, 32  
 Roskar, R., Debattista, V.P., Stinson, G.S., et al. 2008, *ApJ*, 675, L65  
 Santiago, B.X. & Vale, T.B. 2008, *A&A*, 485, 21  
 Sommer-Larsen, J., Götz, M. & Portinari, L. 2003, *ApJ*, 596, 47  
 Teyssier, R. 2002, *A&A*, 385, 337  
 Yoachim, P. & Dalcanton, J. 2006, *AJ*, 131, 226  
 Yoachim, P. & Dalcanton, J. 2008, *ApJ*, 682, 1004